

## Electron and Ion Heat Fluxes in the SOL Plasmas

T.K.Soboleva\*, O.V.Batishchev \*\*, J.J.Martinell\*

\* *Instituto de Ciencias Nucleares, UNAM, Mexico City, Mexico*

\*\* *Massachusetts Institute of Technology, Cambridge MA 02139, USA*

### Introduction

Non-local effects on heat transport were shown to be important for surprisingly low Coulomb Knudsen numbers up to  $10^{-3} - 10^{-2}$  [1]. The reason for that is that Coulomb mean free path is proportional to the second power of the plasma temperature. Therefore, the heat flux is predominantly carried by suprathermal particles [2] (with energies  $\mathcal{E} \sim 6T$ ) as shown in the Fig. 1 below [3,4] by a solid curve.

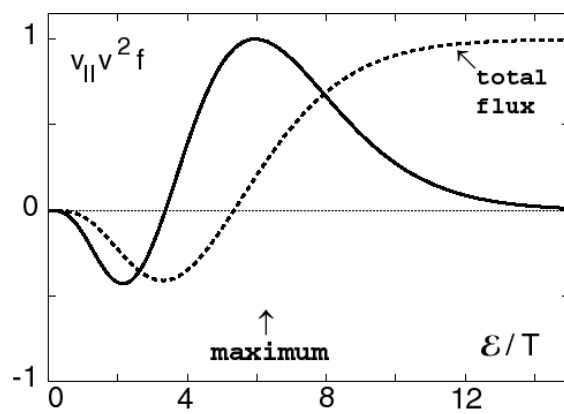


Fig.1

Plasma in magnetic and inertial confinement fusion devices has this number in the range  $10^{-2} - 10^{-1}$  and requires non-local corrections.

However, all existing theoretical studies are limited to either linearized [1] and/or asymptotical [5] models and consider only electron transport. They usually assume that flow is stagnated. Non-linear electron-electron and ion-ion interactions can modify parallel conductivity. Electron-ion energy exchange can be potentially important as

well. In the present work we try to include all these effects self-consistently. The system of equations becomes quite complex. To solve it we use a numerical finite-difference approach, described below.

### Mathematical model

Plasma evolution is described by the following two coupled kinetic equations for electron and ion distribution functions  $f_{e,i}(t, x, v, \mu)$ ,  $\mu = v_x/v$ ,  $v$  - modulus of the velocity.

$$\begin{aligned}
 \frac{\partial f_e}{\partial t} + v\mu \frac{\partial f_e}{\partial x} - \frac{1}{v^2} \frac{\partial}{\partial v} \left[ v^2 \mu \frac{eE_x}{m_e} f_e \right] + \frac{1}{v} \frac{\partial}{\partial \mu} \left[ (1-\mu^2) \frac{eE_x}{m_e} f_e \right] = \\
 C_{ee} + C_{ei} + S_e \tag{1} \\
 \frac{\partial f_i}{\partial t} + v\mu \frac{\partial f_i}{\partial x} + \frac{1}{v^2} \frac{\partial}{\partial v} \left[ v^2 \mu \frac{eE_x}{M_i} f_i \right] - \frac{1}{v} \frac{\partial}{\partial \mu} \left[ (1-\mu^2) \frac{eE_x}{M_i} f_i \right] = \\
 C_{ii} + C_{ie} + S_i
 \end{aligned}$$

where  $E_x$  is a self-consistent electric field,  $C_{\alpha\beta}$  the full non-linear Coulomb collisional terms [6] (which can be easily reduced to a linear, or even simpler – like pitch angle scattering only – model):

$$C_{\alpha\beta} = \frac{L^{\alpha/\beta}}{v^2} \left\{ \frac{\partial}{\partial v} v^2 \left[ \frac{m_\alpha}{m_\beta} \frac{\partial \varphi^\beta}{\partial v} f^\alpha - \frac{\partial^2 \psi^\beta}{\partial v^2} \frac{\partial f^\alpha}{\partial v} - \frac{1-\mu^2}{v^2} \left( \frac{\partial \psi^\beta}{\partial v \partial \mu} - \frac{1}{v} \frac{\partial \psi^\beta}{\partial \mu} \right) \frac{\partial f^\alpha}{\partial \mu} \right] + \frac{\partial}{\partial \mu} (1-\mu^2) \left[ \frac{m_\alpha}{m_\beta} \frac{\partial \varphi^\beta}{\partial \mu} f^\alpha - \left( \frac{\partial^2 \psi^\beta}{\partial v \partial \mu} - \frac{1}{v} \frac{\partial \psi^\beta}{\partial \mu} \right) \frac{\partial f^\alpha}{\partial v} - \left( \frac{1}{v} \frac{\partial \psi^\beta}{\partial v} + \frac{1-\mu^2}{v^2} \frac{\partial^2 \psi^\beta}{\partial \mu^2} - \frac{\mu}{v^2} \frac{\partial \psi^\beta}{\partial \mu} \right) \frac{\partial f^\alpha}{\partial \mu} \right] \right\} \quad (2)$$

the so-called Rosenbluth potentials  $\varphi^\beta$  and  $\psi^\beta$  are obtained from the two linked Poisson equations

$$\nabla^2 \varphi^\beta = f_\beta, \quad \nabla^2 \psi^\beta = \varphi^\beta \quad (3)$$

with asymptotic boundary conditions ( $V \rightarrow \infty$ ):

$$\varphi^\beta(V) = \varphi_M^\beta(V), \quad \psi^\beta(V) = \psi_M^\beta(V), \quad \text{where for } V \gg v_t^\beta \text{ we have used}$$

Maxwellian Rosenbluth potentials

$$\varphi_M^\beta(v) = \frac{n^\beta}{v_t^\beta} \varphi_0 \left( \frac{v}{v_t^\beta} \right), \quad \psi_M^\beta(v) = n^\beta v_t^\beta \psi_0 \left( \frac{v}{v_t^\beta} \right) \quad (4)$$

here  $v_t^\beta = \sqrt{2T_\beta / m_\beta}$  is a thermal velocity of  $\beta$  species. The functions  $\varphi_0$  and  $\psi_0$  in the r.h.s. of Eq. (4) could be easily expressed via error function  $erf$  and its derivative

$$erf(x) = \frac{2}{\sqrt{\pi}} \int_0^x e^{-t^2} dt, \quad erf'(x) = \frac{2}{\sqrt{\pi}} e^{-x^2}, \quad (5)$$

as, respectively,

$$\varphi_0(x) = -\frac{erf(x)}{4\pi x}, \quad \psi_0(x) = -\frac{erf'(x) + (2x + x^{-1}) erf(x)}{16\pi} \quad (6)$$

In the Eq. (1)  $S_\alpha$  are the plasma sink/sources at the boundaries. The geometry of the problem is presented in Fig. 2. At the left ( $x=0$ ) and right ( $x=L$ ) boundaries both electrons and ions, which are continuously "imported" into the system, have Maxwellian distribution with temperatures  $T_L$  and  $T_R$ , respectively. We chose the densities,  $n$ , from the condition  $P=nT \approx const$ . The finite-volume numerical method solving the system (1) is described in detail in ref. [7]. Note that the electric field is strictly ambipolar and the plasma is quasineutral.

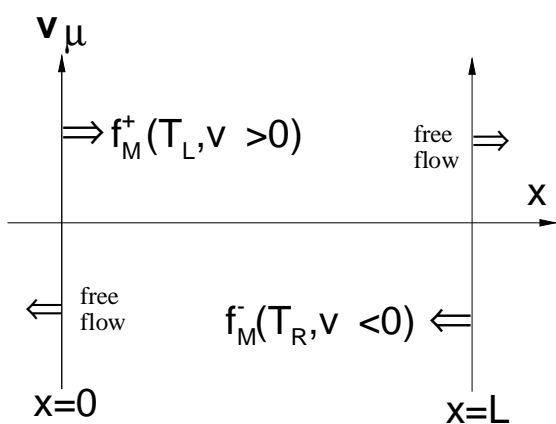


Fig. 2

We performed several runs, in which we have varied the plasma collisionality. The Coulomb Knudsen number,  $K \propto T^2/nL$ , of course, is a function of space. We choose the following parameters:  $L=1m, n(x=0)=10^{13} cm^{-3}, T(x=0)=1eV, T(x=L)=10eV$ . This corresponds to a Knudsen number variation in a reasonable

1/50-1 range.

We have performed three runs: A – with the Maxwellian potentials and arbitrary velocity of a plasma flow, B – the same, but with zero flow velocity, C – same as B but with full Rosenbluth potentials.

**Results**

Our results for the cases A, B, and C using moderate 51x129x33 grid at 0.1ms are shown in the figures below (25mks for C). One can see from the Fig. 3 that the free flow makes ion

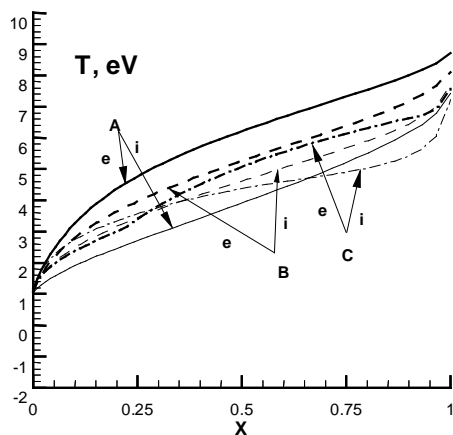


Fig. 3 Electron and ion temperature profiles for the cases A, B and C

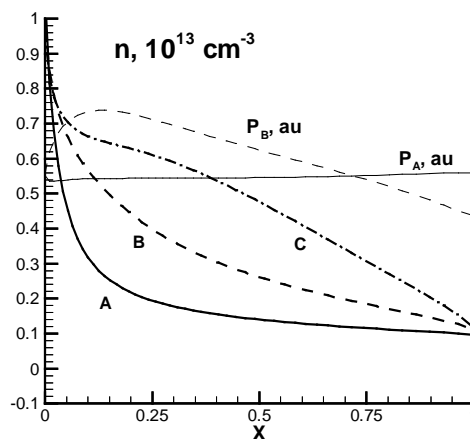


Fig. 4 Plasma density and electron pressure profiles for the cases A, B and C

temperature profile less classical (conductive) than the electron profile. In the non-flow case B electron and ion temperatures are more equilibrated. Density profile is also less peaked in this case (Fig.4). Note that case C may be not fully equilibrated. The total electron pressure in the case A,  $P_A$ , is almost constant, while in case B static pressure,  $P_B$ , is non-uniform.

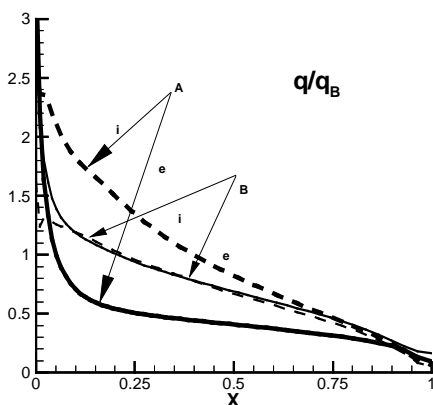


Fig.5 Ratios of the electron and ion heat fluxes to the corresponding Braginskii [8] results

As can be seen from Fig. 5, the heat flux differs from the short mean-free path prescription [8]. In the upper half of the region it is experiencing so-called “flux-limiting” due to the predominant loss of tail particles. Note that the minimum of the ion flux is  $0.1q_B$ , while for the electron flux it’s two times bigger. Maximum of ion flux in the case A is almost two times higher than the electron flux. In the case B both fluxes are almost equal in the whole domain.

Explanation for such behaviour of the heat flux follows from the calculated distribution functions of the plasma species

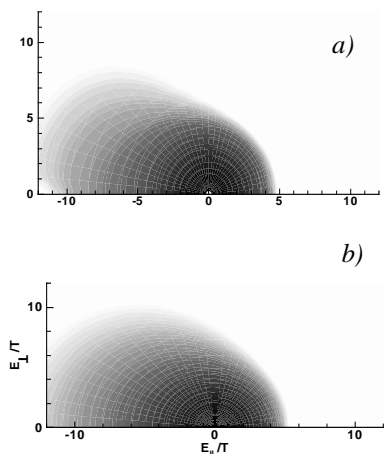


Fig. 6ab Ion (a) and electron (b) distribution functions at 0.1L from the x=0 boundary

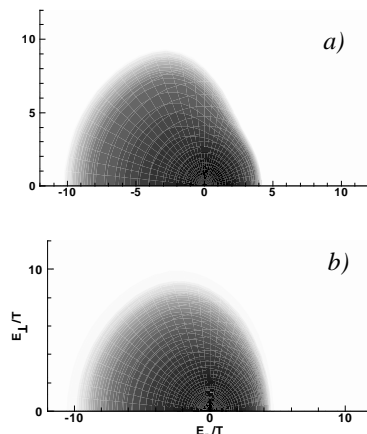


Fig. 7ab Ion (a) and electron (b) distribution functions at 0.3L from the x=L boundary

in the different parts of the domain, as shown in the Fig.6ab and 7ab.

### References

- [1] J. Luciani, P.Mora, J.Virmont, *Phys. Rev. Lett.* **51** (1983) 1664.
- [2] L. Spitzer and R. Harm, *Phys. Rev.* **89** (1953) 977.
- [3] R. Chodura, *Contrib. Plasma Phys.* **28** (1988) 4.
- [4] O. Batishchev et al., *Phys. Plasma* **4** (1997) 1672.
- [5] S. Krasheninnikov, *Phys. Fluids B* **5** (1993) 74.
- [6] B. Trubnikov, in *Rev. Plasma Phys.* (Cons. Bur., NY) vol. 1 (1965) 105.
- [7] O. Batishchev et al., *J. Plasma Phys.*, **61** (1999) 347.
- [8] S. Braginskii, in *Rev. Plasma Phys.* (Cons. Bur., NY) vol. 1 (1965) 205.